SMALL-X PHYSICS AND BFKL DYNAMICS* **

A.H. MUELLER

Department of Physics, Columbia University
New York, N.Y. 10027, USA

(Received November 17, 1997)

After a brief review of the parton model in deep inelastic lepton-proton scattering DGLAP evolution and its relationship to BFKL evolution is discussed. The dipole picture of BFKL evolution is developed in the context of heavy onium-heavy onium scattering. The BFKL evolution equation is derived and solved. At very high energies BFKL behavior leads to scattering cross sections that exceed unitarity limits. A simple picture of unitarity is described in dipole language. Finally, the present state of the experimental search for BFKL evolution is given.

PACS numbers: 12.38. -t, 12.38. Cy

1. Introduction

This written version of two lectures given at the XXXVII Cracow School attempts to furnish an introduction to small-x physics, in particular the small-x physics that relates to Balitsky, Fadin, Kuraev and Lipatov (BFKL) [1,2] evolution. BFKL evolution is particularly interesting because it leads to high density partonic (mainly gluonic) systems where nonlinear QCD effects should become prominent. However, BFKL evolution does not show up so easily in the simplest observables in deep inelastic lepton-proton or hadron-hadron collisions. For that reason it is particularly important to carefully consider where and how to find BFKL evolution as well as to describe the dynamics of BFKL evolution itself.

We begin our discussion with a brief review of deep inelastic lepton-proton scattering and the parton model followed by a description of Dokshitzer, Gribov, Lipatov, Altarelli and Parisi (DGLAP) [3–5] evolution in

* Presented at the XXXVII Cracow School of Theoretical Physics, Zakopane, Poland, May 30–June 10, 1997.

** Work supported in part by the US Department of Energy under Grant No. DE-FG02-94ER 40819.

Section 2. A brief comparison of DGLAP and BFKL evolution is given, and it is noted that the latter is really a part of the former. In Section 3, we describe the dipole picture of BFKL evolution [6–8]. The dipole picture is a particularly simple way of arriving at BFKL evolution in the context of large N_c QCD, although the large N_c limit is not necessary for the main result we aim at. In Section 4 a qualitative discussion is given concerning what happens at very high energies when unitarity corrections to BFKL evolution become important. Finally, in Section 5, we describe how to find BFKL evolution experimentally and the current status of the experimental results.

2. Deep inelastic scattering, the parton model and the DGLAP equation

2.1. Deep inelastic scattering and the parton model

The deep inelastic lepton-nucleon reaction is illustrated in Fig. 1. The cross section for scattering an unpolarized lepton off an unpolarized nucleon is given in terms of structure functions W_1 and W_2 as

$$\frac{d\sigma}{dE'd\Omega'} = \frac{4\alpha_{em}(E')^2}{Q^4}\left[W_2\cos^2\left(\frac{\theta}{2}\right) + 2W_1\sin^2\left(\frac{\theta}{2}\right)\right] \tag{1}$$

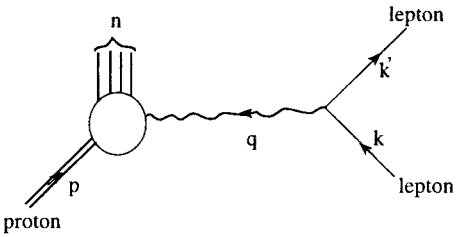

Fig. 1

in the rest frame of the nucleon. E′ is the energy of the outgoing lepton and θ is the angle of scattering between the initial and final lepton directions. α_{em} is the usual fine structure constant and $Q^2 = -q_\mu q_\mu$ is the invariant momentum transfer carried by the virtual photon. W_1 and W_2 are structure functions defined in terms of the structure tensor

$$W_{\mu\nu}(p,q) = \frac{4\pi^2 E_p}{m}\int d^4x\; e^{iqx}(p \mid j_\mu(x)j_\nu(0) \mid p) \tag{2}$$

by

$$W_{\mu\nu} = -\left(g_{\mu\nu} - \frac{q_\mu\, q_\nu}{q^2}\right) W_1 + \frac{1}{m^2}\left[p_\mu p_\nu - \frac{p\cdot q}{q^2}(p_\mu q_\nu + p_\nu\, q_\mu) + \frac{(p\cdot q)^2}{(q^2)^2} q_\mu\, q_\nu\right] W_2\,. \tag{3}$$

In the above m is the nucleon mass, and a spin average over nucleon spin orientations is assumed.

In describing deep inelastic lepton-nucleon scattering in the parton model it is important to refer to a particular frame, the Bjorken or infinite momentum frame, in order that the parton picture be manifest. In that frame the proton and virtual photon momenta take the form

$$p = (p_0, p_x, p_y, p_z) \approx \left(p + \frac{m^2}{2p}, 0, 0, p\right) \tag{3a}$$

and

$$q = (q_0, \underline{q}, q_z = 0) \tag{3b}$$

as p becomes arbitrarily large. In terms of the two invariants Q^2 and $\nu = \frac{p\cdot q}{m}$ one finds $q_0 = \frac{m\nu}{p}$ which becomes small as p becomes large so that $\underline{q}^2 = Q^2$ as $p \to \infty$. In what follows we shall generally take Q^2 and $x = \frac{Q^2}{2p\cdot q}$ as the two independent invariants on which W_1 and W_2 can depend.

In discussing the physical basis of the parton model it is useful to consider $T_{\mu\nu}$ defined as in (2) but with $j_\mu(x)j_\nu(0)$ replaced by $T(j_\mu(x)j_\nu(0))$ with T the usual time-ordering symbol. Then

$$W_{\mu\nu} = 2\mathrm{Im}T_{\mu\nu}\,, \tag{4}$$

where $T_{\mu\nu}$ is forward elastic scattering amplitude for virtual photons on a proton.

To arrive at the parton model it is necessary to consider the time evolution of the proton state in the interaction picture. The proton consists of three valence quarks along with a quark- antiquark sea and gluons. The sea quarks and gluons are created and reabsorbed with the passage of time. In the proton's rest system the typical time between interactions should be $1/\Lambda$ since $\Lambda \approx 200$ MeV is the only genuine scale in light quark QCD. In the Bjorken frame, we can expect this scale to be time-dilated so that $\frac{p}{m\Lambda}$ becomes the natural scale for virtual fluctuations. Now the lifetime of the virtual photon, the time between its emission by the lepton and its absorption by a quark, is given by

$$\tau_\gamma = \frac{1}{|\,\underline{q}\,| - q_0} \approx \frac{1}{Q} << \frac{p}{m\Lambda} \tag{5}$$

in the Bjorken frame. Thus one may view the photon as being absorbed instantaneously by some quark in the proton so long as we use the Bjorken frame.

Suppose the quark which absorbs the photon has longitudinal momentum k. Then, upon absorbing the virtual photon, the struck quark becomes highly virtual with a lifetime of size $\frac{k}{Q^2}$, and since this time is much shorter than the normal interaction time between quarks in the proton the struck quark must re-emit the photon before an interaction with the other quarks and gluons in the proton take place. Finally, since the transverse momentum of the absorbed photon is $\mid \underline{q} \mid = Q$ the photon must be absorbed, and re-emitted, over a transverse coordinate region $\Delta x_\perp \approx \frac{1}{Q}$. That is the quark which absorbs the virtual photon, the struck quark having longitudinal momentum fraction $k = xp$, is pointlike (bare) down to a transverse size $\Delta x_\perp \approx \frac{1}{Q}$.

Thus, our picture of $T_{\mu\nu}$, and from (4) of $W_{\mu\nu}$, is that the scattering by the virtual photon takes place essentially instantaneously and over a very small, almost pointlike, spatial region. Since the photon interacts only with a single quark we expect $T_{\mu\nu}$, and $W_{\mu\nu}$, to be given in terms of number densities of quarks in the proton times the $T_{\mu\nu}$, or $W_{\mu\nu}$, of a single quark. We stress that this physical picture of deep inelastic scattering as a measurement of the number density of quarks in the wavefunction of the proton only holds in the infinite momentum frame of the proton. In terms of formulas

$$\nu W_2(x, Q^2) = \sum_f e_f^2 x P_f(x, Q^2) \,, \tag{6}$$

where $P_f(x, Q^2)$ is the number density of quarks, or antiquarks, in the proton and e_f is the change, in units of the proton's charge.

2.2. The DGLAP equation

The formula given in (6) is valid in the (QCD improved) parton model. At higher orders in $\alpha(Q)$ there are corrections to (6) which are systematically described by the DGLAP equation. In order to describe this write, in general,

$$\nu W_2(x, Q^2) = \sum_{i=f,\bar{f},q} \int_x^1 dx' P_i(x', Q^2) E_i\left(\frac{x}{x'}, \alpha(Q)\right), \tag{7}$$

where the coefficient function is calculable, order by order in $\alpha(Q)$,

$$E_i(x, \alpha) = e_i^2 \delta(x-1) + \alpha E_i^{(1)}\left(\frac{x}{x'}, \alpha\right) + \cdots \tag{8}$$

and where the parton densities obey the DGLAP equation

$$Q^2 \frac{\partial}{\partial Q^2} P_i(x, Q^2) = \sum_j \int_x^1 \frac{dx'}{x'} \gamma_{ij}\left(\frac{x}{x'}, \alpha(Q)\right) P_j(x', Q^2). \tag{9}$$

The anomalous dimension matrix also can be expanded in powers of $\alpha(Q)$ as

$$\gamma_{ij}(x, \alpha) = \alpha \left[\gamma_{ij}^{(0)}(x) + \alpha \gamma_{ij}^{(1)}(x) + \cdots\right]. \tag{10}$$

The standard procedure for describing deep inelastic scattering is to evaluate $\gamma_{jk}(x, \alpha)$ up to a given order and solve for $P_i(x, Q^2)$ using (9) in terms of $P_i(x, Q_0^2)$ for some chosen Q_0^2. Calculating E_i to the corresponding order allows one to calculate $\nu W_2(x, Q^2)$ in terms of the initial distribution $P_i(x, Q_0^2)$ which is then fit to data. For example, if one takes only the α term in γ_{ij} and the lowest order term in E_i one obtains the QCD improved parton model as the *first order* DGLAP analysis. Taking the α and α^2 terms of γ_{ij} and the α^0 and α terms in E_i is the *second order* DGLAP analysis, and this is the level at which one currently works. In the not too distant future we can expect a third order DGLAP analysis to become the standard. This procedure works very well so long as x is not too small. However, there are terms in $\gamma_i^{(n)}(x)$ of size $\left(\ln \frac{1}{x}\right)^{n-1}$ so that when $\alpha(Q) \ln \frac{1}{x}$ is of order one we must expect that the standard ordering in DGLAP analyses will break down. The procedure must be modified when $\alpha \ln\left(\frac{1}{x}\right)$ is of order one. In that case, one writes [9–12]

$$\gamma(\alpha, x) = \alpha \sum_{n,r=0}^{\infty} \alpha^r \left(\alpha \ln \frac{1}{x}\right)^n \gamma^{(r,n)}. \tag{11}$$

The series $\gamma^{(0,n)}$ is known and we can soon expect to have $\gamma^{(1,n)}$ which will put resumed perturbation theory on the same footing as the standard DGLAP analysis [13–16].

DGLAP analyses apply to problems having two transverse momentum scales. For deep inelastic scattering there is the scale Λ coming from the details of the soft structure of the proton while the hard scale q^2 is set by the virtual photon probe. BFKL evolution, on the other hand, applies, in its most straightforward way, only to problems having a single transverse momentum and only when that scale is hard. Thus, for example, the high energy dependence of the total virtual photon-virtual photon cross section, $\gamma^*(Q) + \gamma^*(Q) \to$ hadrons [17–20], is such a process. Later we shall describe processes, for which preliminary measurements already exist at Fermilab and HERA, where BFKL dynamics determines the energy dependence. From

a theoretical point of view the simplest laboratory for describing BFKL dynamics is in high energy heavy onium-heavy onium scattering [6–8]. The single transverse momentum scale is given by the inverse radius of the onium which is large when the heavy quark mass is sufficiently large.

3. The dipole picture of BFKL evolution

3.1. Lowest order

At lowest order the cross section for heavy onium-heavy onium scattering is given in terms of the amplitude illustrated in Fig. 2, where the lines $P-k_1$ and $P'-k_1'$ are heavy quarks and the lines k_1 and k_1' are heavy antiquarks.

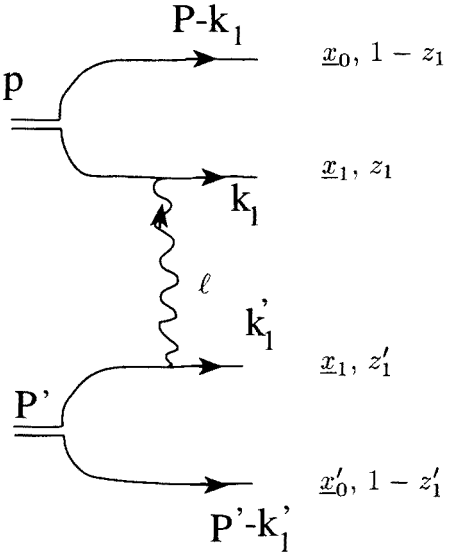

Fig. 2

We find it convenient to describe the onium wavefunctions using transverse coordinate space variables, $\underline{x}_0, \underline{x}_1, \underline{x}_0', \underline{x}_1'$, and longitudinal momentum fractions, $z_1, 1-z_1, z_1', 1-z_1'$, as indicated in Fig. 2. The coordinate and momentum space wavefunctions are related by

$$\psi^{(0)}(x_{01}, z_1) = \int \frac{d^2k_1}{(2\pi)^2} e^{i\underline{k}_1 \cdot \underline{k}_{01}} \psi^{(0)}(k_1, z_1)\,, \tag{12}$$

where $\underline{x}_{01} = \underline{x}_1 - \underline{x}_0$ and the superscript (0) indicates a lowest order (no soft gluons) wavefunction. In terms of $\Phi^{(0)} = \mid \psi^{(0)} \mid^2$ the lowest order cross

section is

$$\sigma^{(0)} = \int d^2x_{01} \int_0^1 dz_1 \Phi^{(0)}(x_{01}, z_1) \int d^2x'_{01} \int_0^1 dz'_1 \Phi^{(0)}(x'_{01}, z'_1) \sigma_{dd}(x_{01}, x'_{01}) \,, \tag{13}$$

where σ_{dd} is the dipole-dipole scattering cross section

$$\sigma_{dd}(x, x') = 2\pi\alpha^2 x_<^2 \left(1 + \ln \frac{x_>}{x_<}\right) \tag{14}$$

with $x_>$ the greater of x and x' and with $x_<$ the lesser. Our normalization is such that

$$\int d^2x \int_0^1 dz \Phi^{(0)}(x, z) = 1 \,. \tag{15}$$

Problem 1 : *Show*

$$\sigma_{dd}(x_{01}, x'_{01}) = \alpha^2 \int \frac{d^2\ell}{[\ell]^2} (2 - e^{i\underline{\ell}\cdot\underline{x}_{01}} 7 - e^{-i\underline{\ell}\cdot\underline{x}_{01}})(2 - e^{i\underline{\ell}\cdot\underline{x}'_{01}} - e^{-i\underline{\ell}\cdot\underline{x}'_{01}})$$

and use

$$\int_0^\infty \frac{d\ell}{\ell^3} (1 - J_0(\ell x))(1 - J_0(\ell x')) = \frac{1}{4} x_<^2 \left(1 + \ln \frac{x_>}{x_<}\right)$$

to get (14) when orientations of $\underline{x}_{01}$ *and* $\underline{x}'_{01}$ *are averaged over.*

3.2. One soft gluon in the wavefunction

The onium wavefunction having a single soft gluon, along with the heavy quark- antiquark, is calculated from the graphs in Fig. 3, where softness means $z_2 << 1$. In the large N_c limit the emission of a gluon changes a dipole into two dipoles. The original dipole, the heavy quark-antiquark pair, becomes two dipoles consisting of the heavy quark and the antiquark part of the gluon making up the first dipole and the quark part of the gluon along with the heavy antiquark making up the second dipole. We illustrate the sum of the two graphs in Fig. 3 by the single graph of Fig. 4 where the dipole structure is emphasized.

In order to derive the BFKL equation one needs only to calculate the graphs of Fig. 3 in lightcone gauge where the polarization of the gluon is

$$\varepsilon_\mu^\lambda(k) = (\varepsilon_+^\lambda, \varepsilon_-^\lambda, \underline{\varepsilon}^\lambda) = \left(0, \frac{\underline{\varepsilon}^\lambda \cdot \underline{k}}{k_+}, \underline{\varepsilon}^\lambda\right). \tag{16}$$

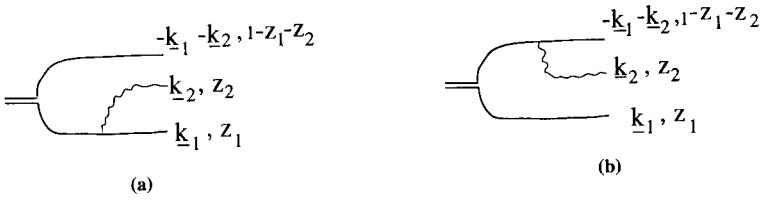

Fig. 3

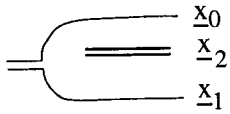

Fig. 4

In the soft gluon approximation, which corresponds to the usual leading logarithmic approximation in which BFKL dynamics is formulated, one need only keep ε_-^λ in (16) because the $1/k_+$ is a large quantity. Using the fact that the ε_- polarization couples to the classical current of a high momentum quark or antiquark we can immediately write down the contribution of the graphs in Fig. 3 to the wavefunction of the onium as

$$\psi^{(1)}(k_1,k_2,z_1,z_2)=gT^a\frac{1}{\underline{k}_2^2/2k_{2+}}\frac{\underline{\varepsilon}^\lambda\cdot\underline{k}_2}{k_{2+}}(\psi^{(0)}(k_1+k_2,z)-\psi^{(0)}(k_1,z_1))\,, \tag{17}$$

where T^a is the color matrix for a gluon of color a, and $[\underline{k}_2^2/2k_{2+}]^{-1}$ is the energy denominator which is dominated by the soft gluon. Going to transverse coordinate space by

$$\psi^{(1)}(x_{02},x_{21},z_1,z_2)=\int\frac{d^2k_1d^2k_2}{(2\pi)^4}e^{i\underline{k}_1\cdot\underline{x}_{01}+i\underline{k}_2\underline{x}_{02}}\psi^{(1)}(k_1,k_2,z_1,z_2) \tag{18}$$

one finds, using (17),

$$\psi^{(1)}(x_{02},x_{21},z_1,z_2)=\psi^{(0)}(x_{01},z_1)\frac{igT^a}{\pi}\left(\frac{\underline{x}_{02}}{x_{02}^2}+\frac{\underline{x}_{21}}{x_{21}}\right). \tag{19}$$

Squaring and taking a trace over colors gives

$$\Phi^{(1)}=\Phi^{(1)}(x_{01},z_1)\frac{2\alpha N_c}{\pi}\,\frac{x_{01}^2}{x_{12}^2x_{02}^2}\,. \tag{20}$$

In obtaining (20) we have taken $C_F=N_c/2$ in the large N_c limit.

Problem 2: *Show*

$$\sum_{\lambda}\left[\underline{\varepsilon}^{\lambda}\cdot\left(\frac{\underline{x}_{02}}{x_{02}^2}+\frac{\underline{x}_{21}}{x_{21}^2}\right)\right]^2=\frac{x_{01}^2}{x_{12}^2x_{02}^2}\,.$$

Including a phase space factor

$$d\Omega=\frac{d^2x_2}{2\pi}\,\frac{dz_2}{2z_2}$$

one arrives at the factor

$$\frac{1}{\Phi^{(0)}}\,\Phi^{(1)}d\Omega=\frac{\alpha N_c}{2\pi^2}\,\frac{x_{01}^2d^2x_2}{x_{12}^2\,x_{02}^2}dy_2 \tag{21}$$

as the probability of emitting a soft gluon, and where we have defined $dy_2 = dz_2/z_2$. Eq. (21) is illustrated in Fig. 4.

3.3. Arbitrary numbers of soft gluons

Once a single soft gluon emission has been calculated it is straightforward to add more, even softer gluons. The time sequence for soft gluons to appear in the wavefunction follows their longitudinal momentum. The hardest of the soft gluons appears first, then the next hardest of the soft gluons, *etc.* In each case the emission of a soft gluon creates a transition from a color dipole to two color dipoles with the probability factor given by (21). In order to express this most succinctly it is convenient to introduce a generating functional, Z, obeying

$$Z(x_{01}Y,u)=\exp\left[-\frac{2\alpha N_c}{\pi}Y\ln\left(\frac{x_{01}}{\rho}\right)\right]u(x_{01})+\frac{\alpha N_c}{2\pi^2}$$

$$\times\int_R\frac{x_{01}^2\,d^2x_2}{x_{02}^2\,x_{12}^2}\int_0^Y dy\exp\left[-\frac{2\alpha N_c}{\pi}(Y-y)\ln\left(\frac{x_{01}}{\rho}\right)\right]Z(x_{02},y,u)Z(x_{21},y,u). \tag{22}$$

R is a cutoff and indicates that one take $x_{02}>\rho, x_{12}>\rho$ as the region of integration. Eq. (22) is illustrated in Fig. 5. Z is the generating functional for soft gluons and has the following properties:

$$\frac{\delta}{\delta u(\Delta x_1)}\,\frac{\delta}{\delta u(\Delta x_2)}\cdots\frac{\delta}{\delta u(\Delta x_n)}Z\mid_{u=0} \tag{23}$$

gives, when multiplied by $\Phi^{(0)}(x_{01}, z_1)$ the exclusive probability of having $n-1$ soft gluons in the onium wavefunction with the soft gluons and the heavy quark-antiquark pair making up n dipoles of sizes $\Delta x_1, \Delta x_2, \cdots$. If one takes $u = 1$, rather than $u = 0$, the expression (23) becomes the inclusive probability of having $n-1$ measured soft gluons, along with an arbitrary number of unmeasured gluons, in the onium wavefunction. Finally,

$$Z(x_{01}, Y, u) \mid_{u=1} = 1 \tag{24}$$

is probability conservation and is obtained by including the probability conserving exponential factors in (22) which correspond to virtual loop corrections in the wavefunction [21].

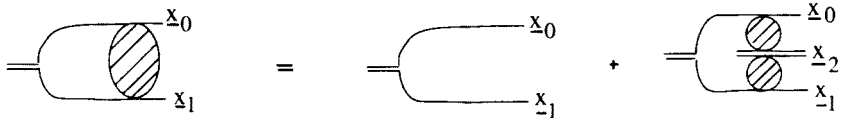

Fig. 5

Problem 3 : *Show that the virtual corrections, the terms in the exponentials in (22) can be obtained using probability conservation by integrating single gluon emission over the available (cutoff) phase space. That is*

$$\frac{\alpha N_c}{2\pi^2} \int_R \frac{x_{01}^2 d^2x_2}{x_{02}^2\, x_{12}^2} \int_0^Y dy = \frac{2\alpha N_c}{\pi} Y \ln \frac{x_{01}}{\rho} + O(\rho^2) .$$

In summary (22) represents the soft gluon wavefunction of a high energy heavy onium. The longitudinal momentum integrations have been done in a leading logarithmic approximation, while the transverse integrations have been handled exactly. The cutoff ρ will disappear when a physical problem is considered. The large N_c limit is essential to obtain (22).

3.4. Scattering in the BFKL approximation

In terms of the heavy onia lightcone wavefunctions, high energy onium-onium scattering is very simple and is reminiscent of partonic expressions in hard scattering. Suppose the scattering takes place in the center of mass.

Then the scattering proceeds by the interaction (scattering) of a single dipole in the left-moving onium with a single dipole in the right-moving onium as illustrated in Fig. 6. The equation is

$$\sigma(Y) = \int \frac{d^2x d^2x'}{4\pi^2 x^2 (x')^2} N\left(x, \frac{Y}{2}\right) N\left(x', \frac{Y}{2}\right) \sigma_{dd}(x, x') , \tag{25}$$

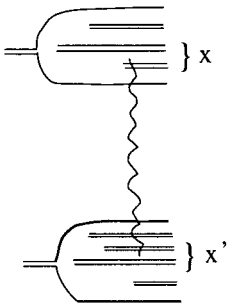

Fig.6

where $N(x,Y)$ is the number density of dipoles of size x, in a rapidity interval Y, in the onium wavefunction. More explicitly,

$$N(x,Y) = \int d^2x_{01}dz_1\Phi^{(0)}(x_{01},z_1)n(x_{01},x,Y) \tag{26}$$

with

$$n(x_{01},x,Y) = x^2\int d\phi(\underline{x})\frac{\delta Z(x_{01},Y,u)}{\delta u(x)}\,|_{u=1}\,, \tag{27}$$

where $d\phi(\underline{x})$ indicates an integration over the orientations of the dipole direction $\underline{x}$. n obeys the dipole version of the BFKL equation

$$\begin{aligned} n(x_{01},x,Y) \;=\; & x\delta(x-x_{01})\exp\left[-\frac{2\alpha N_c}{\pi}Y\ln\frac{x_{01}}{\rho}\right] + \frac{\alpha N_c}{\pi^2}\int\limits_R \frac{x_{01}^2\,d^2x_2}{x_{12}^2\,x_{02}^2} \\ & \times\int\limits_0^Y dy\;\exp\left[-\frac{2\alpha N_c}{\pi}(Y-y)\ln\frac{x_{01}}{\rho}\right]n(x_{12},x,y) \end{aligned} \tag{28}$$

illustrated in Fig. 7.

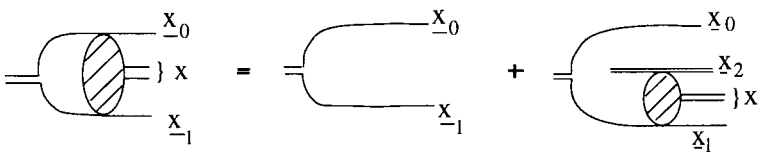

Fig. 7

Problem 4 : *Use (22) and (27) to derive (28).*

In order to solve (28) it is convenient to write it as an evolution equation in Y. Taking a Y-derivative on both sides of (28) gives

$$\frac{d}{dY}n(x_{01},x,Y)=\frac{2\alpha N_c}{\pi}\int_0^\infty dx'_{12}K(x_{01},x'_{12})n(x'_{12},x,Y) \tag{29}$$

with

$$K(x_{01},x'_{12})=\frac{1}{2\pi}\int_R d^2x_2\ \delta(x_{12}-x'_{12})\Big\{\frac{x_{01}^2}{x_{12}^2\ x_{12}^2}-2\pi\delta(\underline{x}_2-\underline{x}_0)\ln\Big(\frac{x_{01}}{\rho}\Big)\Big\}. \tag{30}$$

The limit $\rho\to 0$ can be taken in (30) leaving K a scale covariant kernel. Thus

$$\int dx_{12}K(x_{01},x_{12})x_{12}^{1+2i\nu}=\chi(\nu)x_{01}^{1+2i\nu} \tag{31}$$

from the scale covariance. Explicit calculation [6] gives

$$\chi(\nu)=\psi(1)-\tfrac{1}{2}\psi(\tfrac{1}{2}+i\nu)-\tfrac{1}{2}\psi(\tfrac{1}{2}-i\nu)\,, \tag{32}$$

thus proving that K is the usual BFKL kernel in a different guise. Using (31) in (29) gives

$$n(x_{01},x,Y)=c\int_{-\infty}^{\infty}\frac{d\nu}{2\pi}\Big(\frac{x_{01}}{x}\Big)^{1+2i\nu}e^{\frac{2\alpha N_c}{\pi}\chi(\nu)Y}\,. \tag{33}$$

Problem 5 : *Use $n(x_{01},x,0)=x\delta(x_{01}-x)$ to show that $c=2$ in (33).*

Problem 6 : *Use the fact that $\nu=0$ is a saddle point of $\chi(\nu)$, along with the results $\chi(0)=2\ln 2$ and $\chi''(0)=-14\zeta(3)$, to get*

$$n(x_{01},x,Y)=\frac{x_{01}}{2x}\frac{e^{(\alpha_P-1)Y}}{\sqrt{\frac{7}{2}\alpha N_c\zeta(3)Y}}\ \exp\left[-\frac{\pi\ln^2\left(\frac{x_{01}}{x}\right)}{14\alpha N_c\zeta(3)Y}\right]. \tag{34}$$

Finally, using (26) and (34) in (25) gives

$$\sigma(Y) = 16\pi\alpha^2 R^2 \frac{e^{(\alpha_P - 1)Y}}{\sqrt{\frac{7}{2}\alpha N_c \zeta(3) Y}} \tag{35}$$

with

$$\alpha_P - 1 = 4\alpha N_c \ln\frac{2}{\pi} \tag{36}$$

and

$$R = \frac{1}{2}\int d^2 x_{01} \int_0^1 dz_1 x_{01} \Phi^{(0)}(x_{01}, z_1)\,. \tag{37}$$

4. Beyond BFKL (unitarity corrections)

From (35) one sees that when $\alpha Y \leq 1$ the onium-onium cross section is small. However, as αY becomes larger than 1 the cross section grows rapidly. We can expect corrections to the BFKL result when $\sigma(Y)$ reaches its geometric value of $2\pi R^2$. This happens when

$$Y \approx \frac{1}{\alpha_P - 1} \ln\left(\frac{1}{\alpha^2}\right). \tag{38}$$

One can get a better estimate of the energies where the BFKL picture breaks down by using a formula for the S-matrix in impact parameter space [6]

$$1 - S(b) = \frac{d\sigma}{d^2 b} = \frac{8\pi\ R^2\alpha^2}{b^2} \ln\left(\frac{b^2}{R^2}\right) e^{(\alpha_P - 1)Y} \frac{\exp[-\frac{\pi \ln^2(b^2/R^2)}{14\alpha N_c \zeta(3) Y}]}{\left[\frac{7}{2}\alpha N_c \zeta(3) Y\right]^{3/2}}, \tag{39}$$

a formula which is valid when $R/b << 1$. Requiring $\mid 1 - S(b) \mid \leq 2$ gives a rigorous argument for the breakdown of the BFKL result when Y exceeds the limit given in (38), a limit which is somewhat modified by the b/R dependence in (39).

One might worry that the neglect of running coupling effects in the whole leading order BFKL approach might be a serious defect of this program. However, the next problem shows that this is not the case.

Problem 7 : *Using the fact that* $b^2 \leq R^2 \exp\sqrt{\frac{14\alpha N_c \zeta(3) Y}{\pi}}$ *from (39), show that the requirement*

$$\frac{\alpha(b) - \alpha(R)}{\alpha(R)} << 1 \text{ leads to the condition } Y << \frac{\pi}{14 N_c \zeta(3) b_0^2 \alpha^3(R)}$$

with $b_0 = \frac{33-2N_f}{12\pi}$. This condition is much weaker than that given in (38), at least for sufficiently small $\alpha(R)$, showing that, in principle, unitarity constraints become important at energies well below those where running coupling effects need to be considered.

4.1. A picture of how unitarity is reached [6, 22, 23]

In order to better appreciate the approach to and the setting in of unitarity limits it may be useful to consider a "nuclear" analogy [22]. Imagine that we are able to control the density of neutrons and protons in a nucleus. The parameter

$$\rho = \frac{3A\sigma_0^{3/2}}{4\pi R^3} \tag{40}$$

is just that density made dimensionless by multiplication by the nucleon-nucleon cross section, σ_0. ρ, as given in (4), is often referred to as the packing fraction of nucleons in the nucleus, A. The total cross section for scattering of two identical nuclei having atomic number A is

$$\sigma_{AA} = A^2\sigma_0 = 4\pi R^2\left(\frac{4\pi}{9}\,\frac{R^4}{\sigma_0^2}\right)\rho^2 \tag{41}$$

in the single scattering approximation. When ρ is sufficiently small, for a fixed nuclear radius R, (41) is a reasonable approximation. However, geometrically $\sigma_{AA} \leq 4\pi R^2$ so that as we increase ρ the unitarity limit will be reached and the single scattering approximation will no longer be valid. If $R^2/\sigma_0 >> 1$ the unitarity limit will be reached for quite small ρ. That is, the nuclei become black even when they have a very small packing fraction. Of course, in this nuclear example the procedure is clear. When ρ grows so that one approaches the unitarity limit two and more scatterings must be added coherently to the single scattering amplitude in order to get the correct (unitary) answer.

The situation for heavy onium-heavy onium scattering is similar. From (25) it is clear that the unitarity limit is reached when the number of dipoles in an onium becomes large. However, the unitarity limit is reached, and exceeded when using (25), not because an error has been made in the calculation of $N(x, Y/2)$ but because multiple scattering must be taken into account. There are, however, two main differences with respect to our nuclear analogy. (*i*) In the nuclear analogy the nucleon-nucleon cross section, σ_0, was taken as a fixed value. In the onium-onium case dipoles, which are the counterpart of the nucleons, have a variable size. (*ii*) The number of dipoles in an onium state fluctuates, and these fluctuations are very large

having a tail which approximately obeys a KNO scaling with an exponential KNO function.

We can illustrate how the multiple scattering must be done in a schematic way [6,23]. The S-matrix for scattering of two onia, say in the center of mass, at relative rapidity Y and at impact parameter b is

$$S(Y,b) = \sum_{\phi} P_{\phi}(Y) e^{-f(\phi)}\,, \tag{42}$$

where ϕ labels the state of the colliding onia in terms of the numbers, positions and orientations of the dipoles in each onium. $P_{\phi}(Y)$ is the probability density for the configuration ϕ while $f(\phi)$ is the sum over all two-body dipole scatterings. So long as f is not too large a given dipole will participate in only one scattering and (42) should be an accurate representation of the S-matrix. Detailed numerical calculations have been done by Salam [23], and I limit the discussion here to the highlights of the results. From (42) the single scattering approximation is

$$S = 1 - \sum_{\phi} P_{\phi}(Y) f(\phi)\,, \tag{43}$$

which leads to the BFKL answer (25) since f only involves a single dipole from each onium. When $f(\phi)$ becomes large, for those configurations not having too small probability P_{ϕ}, one must use (42). At large Y, and at fixed b, $f(\phi)$ becomes large except for rare configurations so that $S(Y,b)$ becomes small and unitarity is reached at that b. Numerical calculations show that although there are strong violations of the BFKL result for small b and at moderate Y, the total cross section given by

$$\sigma = 2\int d^2b(1 - S(Y,b)) \tag{44}$$

follows the BFKL formula up to quite large values of Y [23].

If one expands the exponential in (42) one obtains the Glauber series

$$S(Y,b) = \sum_{n=0}^{\infty} (-1)^n S_n(Y,b)\,, \tag{45}$$

where

$$S_n(Y,b) = \frac{1}{n!}\sum_{\phi} [f(\phi)]^n P_{\phi}(Y)\,. \tag{46}$$

In the BFKL context these formulae do not make a lot of sense because there are rare configurations, ϕ, which have very large $f(\phi)$ giving [6,23]

$$S_n(Y,b) \sim n! \tag{47}$$

so that the Glauber series does not converge. Thus we feel that it is essential to sum the multiple scattering series for each configuration, ϕ, before summing over configurations ϕ. This is what is indicated in (42).

5. Phenomenology

We can hope that in time, with precision data and a completely resumed second order DGLAP formalism, evidence for BFKL dynamics will emerge from the Q^2 and x-dependences of νW_2. However, there are more direct ways to measure BFKL evolution and there is already some evidence available from Fermilab and HERA.

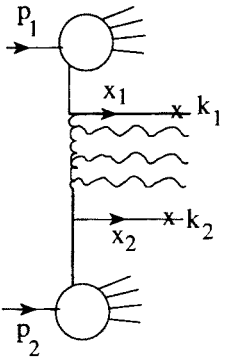

Fig. 8

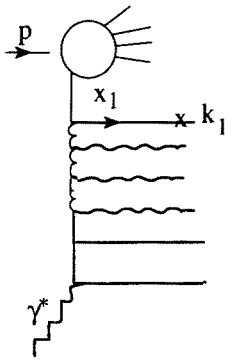

Fig. 9

Inclusive two jet cross sections at Fermilab and forward single jet inclusive cross sections at HERA can be used to measure the BFKL intercept [24–28]. These processes are illustrated in Figs. 8 and 9 respectively

where k_1 and k_2 represent measured jets. In proton-antiproton collisions one chooses $k_{1\perp}, k_{2\perp} > M$, a fixed hard scale while in deep inelastic scattering $k_{1\perp}$ is chosen to be on the order of Q, the photon virtuality. For the hadron-hadron case

$$\sigma_{2-jet} = f(x_1, x_2, M^2) \frac{e^{(\alpha_P - 1)\Delta Y}}{\sqrt{\Delta Y}} \tag{48}$$

while for deep inelastic scattering

$$\sigma_{\rm jet} = f(x_1, Q^2) \frac{e^{(\alpha_P - 1)\ln(x_1/x)}}{\sqrt{\ln\ (x_1/x)}} \tag{49}$$

with x_1 and x_2 being the longitudinal momentum fractions of the measured jets. $\alpha_P - 1 = \frac{4\alpha N_c}{\pi} \ln 2$ and the f's in (48) and (49) are known in terms of the quark and gluon distributions of the proton and antiproton. In (5.1) ΔY is the rapidity difference between the two measured jets. One can get a measurement of $\alpha_P - 1$ in (48) by varying ΔY with x_1, x_2 and M^2 fixed, and this can be done at Fermilab by comparing the inclusive two-jet cross section at different incident energies. In (49) one can measure $\alpha_P - 1$ by varying x for fixed x_1 and Q^2.

Sometime ago H1 [29, 30] presented an analysis showing $\sigma_{\rm jet}$ increasing by about a factor of four as x goes from about 3×10^{-3} to about 7×10^{-4} for $k_{1\perp} > 3.5$ GeV. This is a growth quite a bit faster than given in conventional Monte Carlos and much faster than the growth from single gluon exchange between the measured jet and the quark-antiquark pair coming from the virtual photon. The growth is comparable to that given in (49) for $\alpha_P - 1 \approx 1/2$, however, the comparison is not very convincing because a comparison of partonic energy dependences, from (49), with hadron final states is not very reliable when $k_{1\perp}$ is as small as in the H1 analyses.

Recently, ZEUS [31] has completed an analysis of the process. Since the ARIANDE Monte Carlo gives a good fit to the ZEUS data this Monte Carlo is used to unfold the hadronization and thus get a better comparison with BFKL evolution. The data agree much better with BFKL evolution than with the Born term or with next-to-leading order QCD calculations. A definitive comparison with BFKL dynamics is hindered by the lack of ability to include hadronization corrections along with the BFKL evolution. One can hope that the situation will soon improve in this regard.

A new *DØ* analysis [32] comparing 1800 GeV and 630 GeV data for $k_{1\perp}, k_{2\perp} \geq 20$ GeV gives $\alpha_P = 1.35 \pm 0.04$ (stat) ± 0.22 (syst) when (48) is used to fit the data. The strength of the DØ analysis is that $k_\perp > 20$ GeV which makes uncertainties due to jet definition minimal. Weaknesses of the analysis are the large systematic error and the smallness of ΔY, equal to 2

at the lower energy. We can hope that the systematic error will come down in the near future.

Overall, I think the BFKL searches are encouraging but not yet definitive. The fact that all three analyses suggest a strong increase with energy of reliable quantities for isolating BFKL effects is certainly positive. An attempt will also be made to measure $\alpha_P - 1$ at LEP [33] in the next year by measuring the $\gamma^* - \gamma^*$ total cross section. This is a very clean process, although the cross section is rather small.

REFERENCES

[1] E.A. Kuraev, L.N. Lipatov, V.S. Fadin, *Sov.Phys. JETP* **45**, 199 (1978).
[2] Ya.Ya. Balitsky, L.N. Lipatov, *Sov. J. Nucl. Phys.* **28**, 22 (1978).
[3] Yu.L. Dokshitzer, *Sov. Phys. JETP* **73**, 1216 (1977).
[4] V.N. Gribov, L.N. Lipatov, *Sov. J. Nucl. Phys.* **15**, 78 (1972).
[5] G. Altarelli, G. Parisi, *Nucl. Phys.* **B126**, 298 (1977).
[6] A.H.Mueller, *Nucl. Phys.* **B415**, 373 (1994); **B437**, 107 (1995).
[7] A.J. Mueller, B. Patel, *Nucl. Phys.* **B425**, 471 (1994).
[8] N. Nikolaev, B.G. Zakharov, V.R. Zoller, *JETP Lett.* **59**, 6 (1994).
[9] T.Jaroszewicz, *Phys. Lett.* **B116**, 291 (1982).
[10] S. Catani, F. Hautmann, *Nucl. Phys.* **B427**, 475 (1994).
[11] S. Catani, *Z. Phys.* **C70**, 263 (1996).
[12] R.S. Thorne, *Phys. Lett.* **B392**, 463 (1997).
[13] V.S. Fadin, L.N. Lipatov, *Yad. Fiz.* **50**, 1141 (1989); *Nucl.Phys.* **B406**, 259 (1993); *Nucl. Phys.* **B477**, 767 (1996).
[14] V.S. Fadin, R. Fiore, M.I. Kotsky, *Phys. Lett.* **B359**, 181 (1995); **B387**, 593 (1996); **B389**, 737 (1996).
[15] G. Camici, M. Ciafaloni, *Phys. Lett.* B386, 341 (1996); **B395**, 118 (1997).
[16] G. Camici, M. Ciafaloni, *Nucl. Phys.* **B496**, 305 (1997).
[17] I.F. Ginsburg, S.L. Panfil, V.G. Serbo, *Nucl. Phys.* **B284**, 685 (1987).
[18] S.J. Brodsky, F.Hautmann, D.E. Soper, *Phys. Rev. Lett.* **78**, 803 (1997).
[19] J.Bartels, A. De Roeck, H. Lotter, *Phys. Lett.* **389**, 742 (1996).
[20] A.De Roeck, C. Royon, S. Wallon (in preparation).
[21] Z. Chen, A.H. Mueller, *Nucl. Phys.* **B451**, 579 (1995).
[22] Yu.Kovchegov,A.H. Mueller, S. Wallon, *Nucl. Phys.* **B** (to be published).
[23] G.P. Salam, *Nucl. Phys.* **B461**, 512 (1996).
[24] A.H. Mueller, H. Navelet, *Nucl. Phys.* **B282**, 727 (1987).
[25] W.-K. Tang, *Phys. Lett.* **B278**, 363 (1991).
[26] J. Bartels, A. De Roeck, M. Loewe, *Z. Phys.* **C54**, 635 (1992).
[27] J. Kwiecinski, A.D. Martin, P.J. Sutton, *Phys. Rev.* **D46**, 921 (1992).
[28] V.Del Duca, hep-ph/9707348.

[29] S. Aid *et al.*, H1 Collaboration, *Phys. Lett.* **B35**, 118 (1995).
[30] M. Wobisch for the H1 Collaboration in DIS 1997.
[31] ZEUS Collaboration, contribution to EPS 1997.
[32] A. Goussiou in presentation for the DØCollaboration at EPS 1997.
[33] A.De Roeck, private communication.